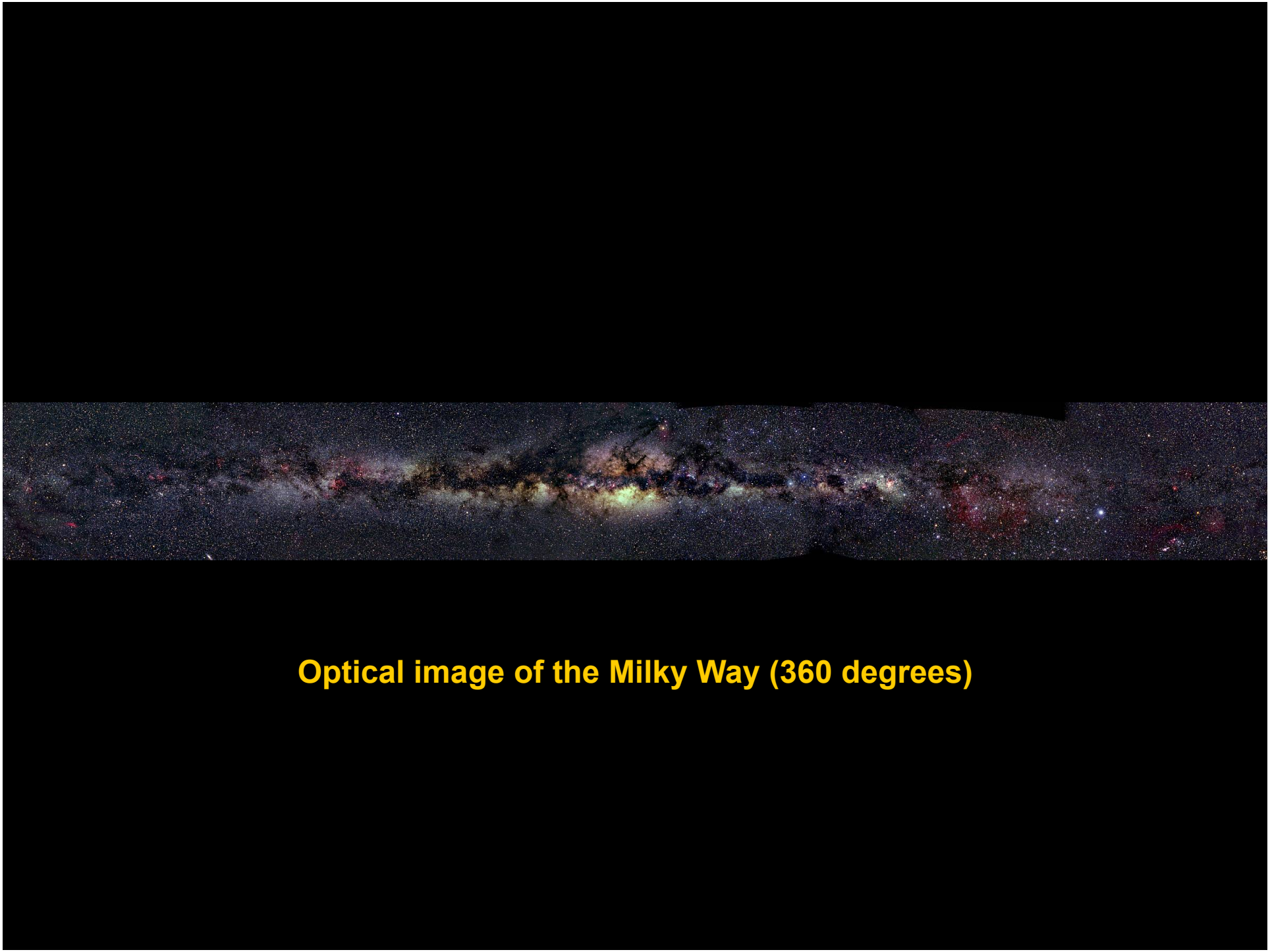

Optical image of the Milky Way (360 degrees)

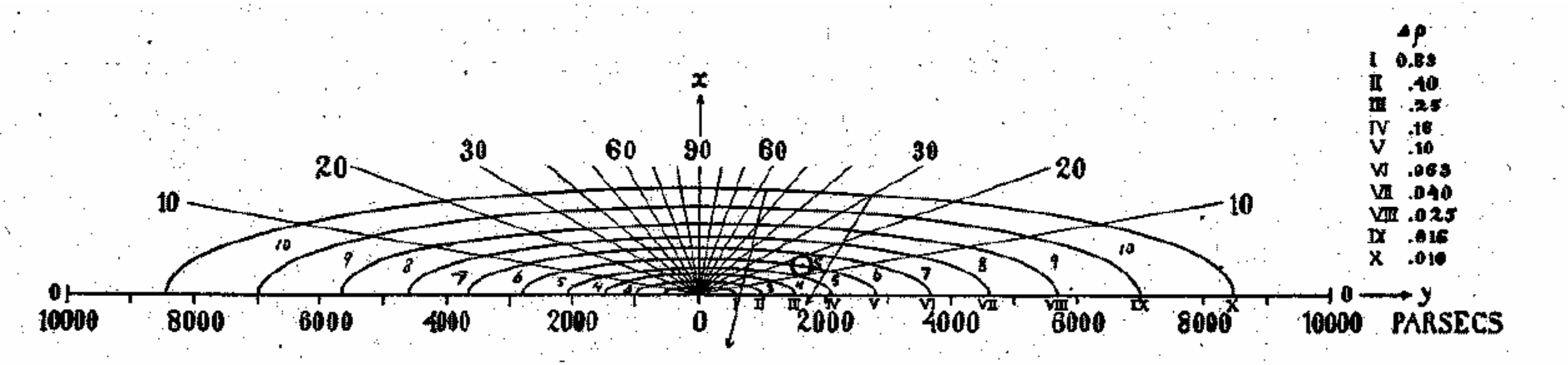

FIG. 1

Kapteyn (1922)

the earlier plot; they are now computed and entered in the third column of Table III. All globular clusters are represented in the new diagram, including the five unproved objects marked with the double dagger in Table II. The open circles designate clusters for which the provisional distances are marked in Table II by a colon.

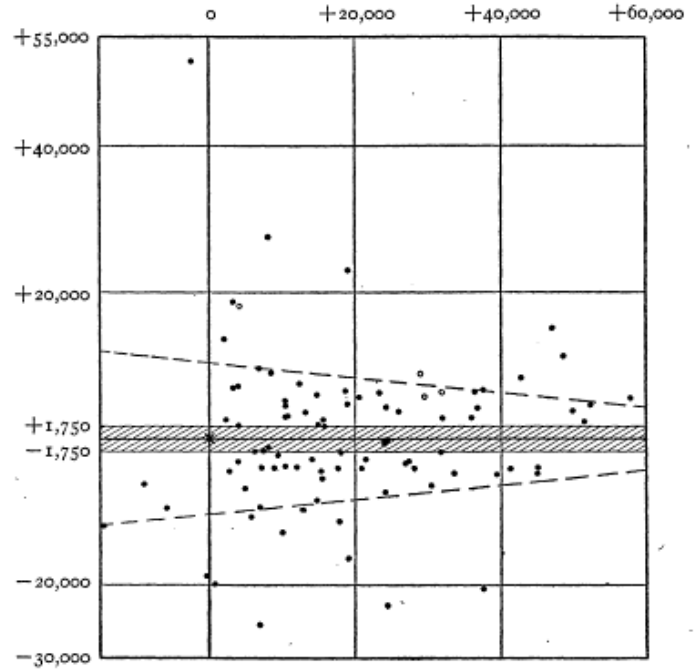

FIG. 3.—Projection of the complete system of globular clusters on a plane perpendicular to the Galaxy and oriented to include the line from the sun to the center of the system. Ordinates are $R \sin \beta$; abscissae are $R \cos \beta \cos (\lambda - 325^\circ)$; unit of distance is one parsec. The sun at the origin of co-ordinates is marked by a cross. See Fig. 4 of *Mt. Wilson Contr.* No. 152.

The parallax of Messier 22 (N.G.C. 6656) has been increased slightly over the value previously adopted. The cluster is fairly open and in a rich field, and it is now found that the stars selected for the study of magnitudes were so near the center that an error of 0.15 mag., due to the Eberhard effect, crept into the earlier results. The values of the galactic co-ordinates for some of the

Shapley (1919)

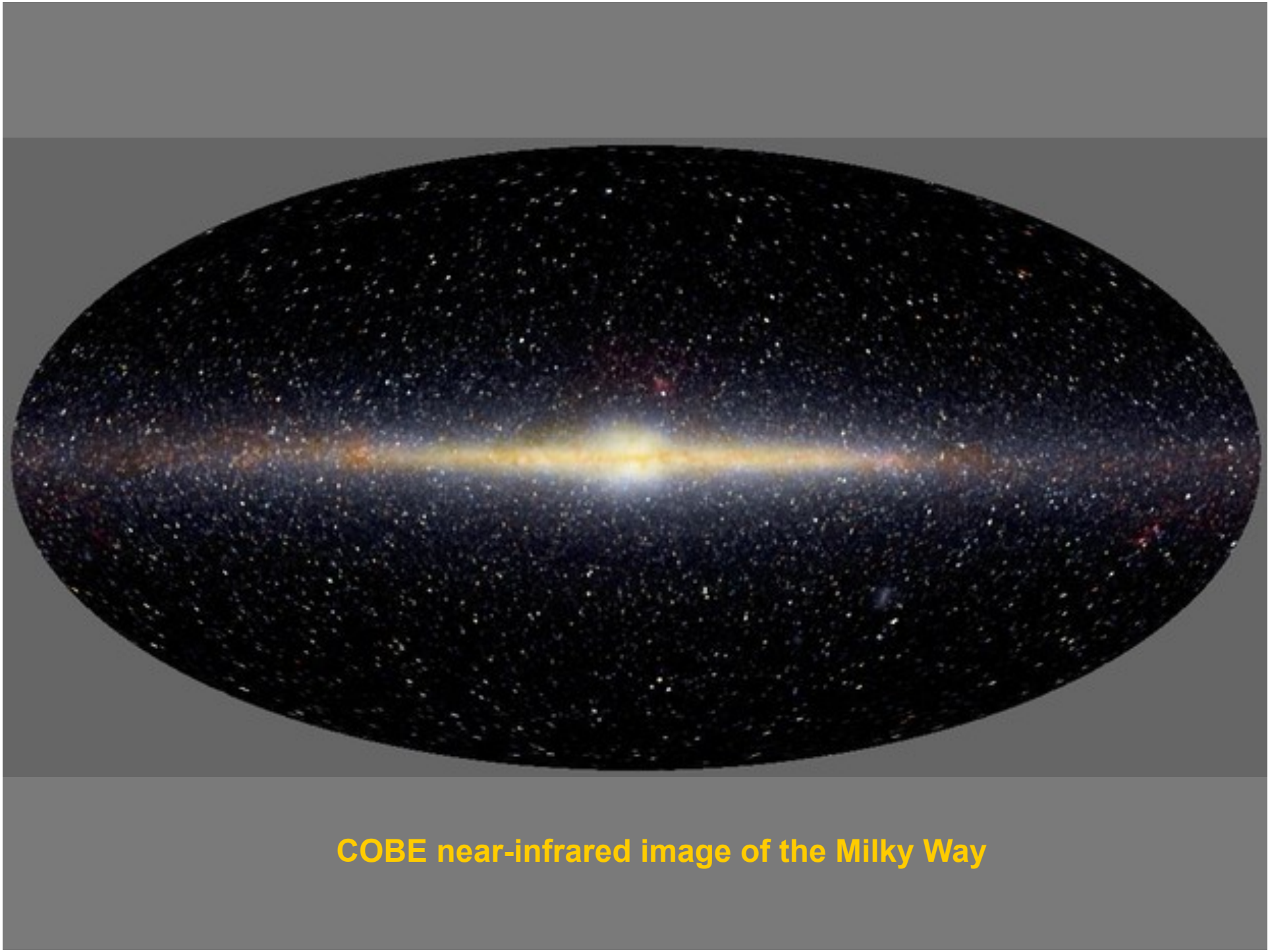

COBE near-infrared image of the Milky Way

2MASS Showcase

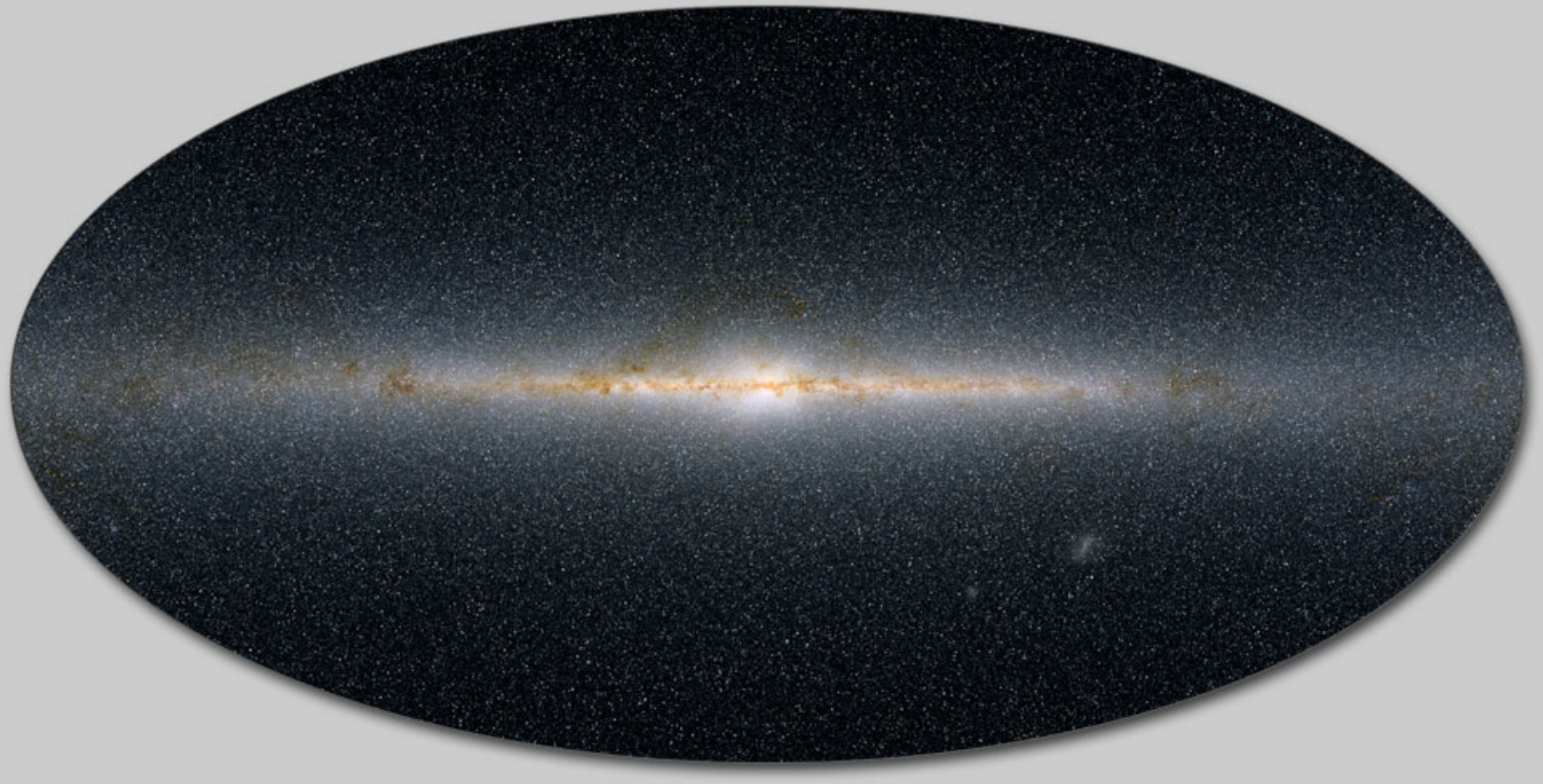

The Infrared Milky Way This map of the infrared sky includes the light of a half billion stars

Two Micron All Sky Survey Image Mosaic: Infrared Processing and Analysis Center/Caltech & University of Massachusetts

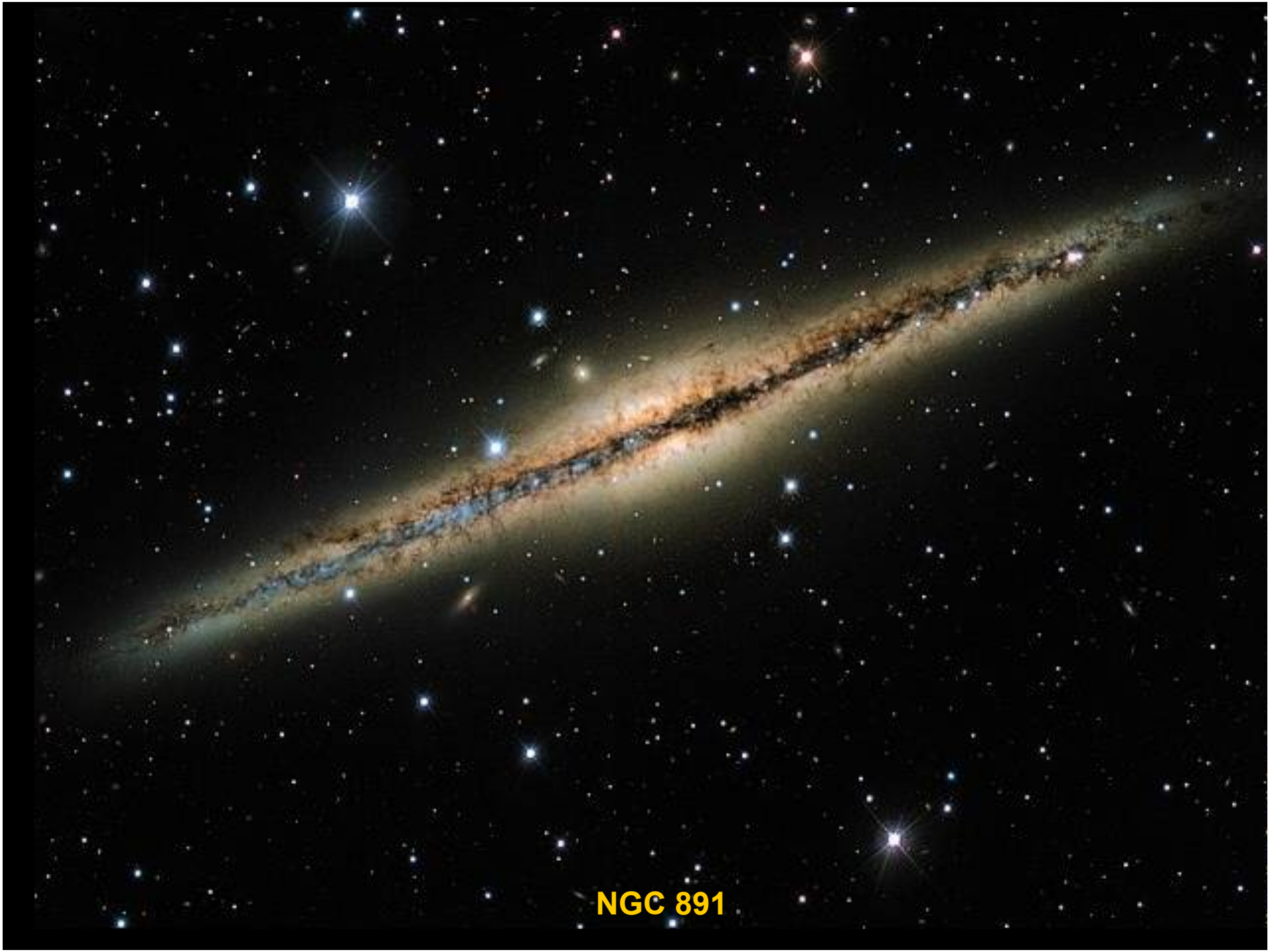
NGC 891


Magellanic
clouds

Fornax dwarf galaxy

Leo I dwarf galaxy

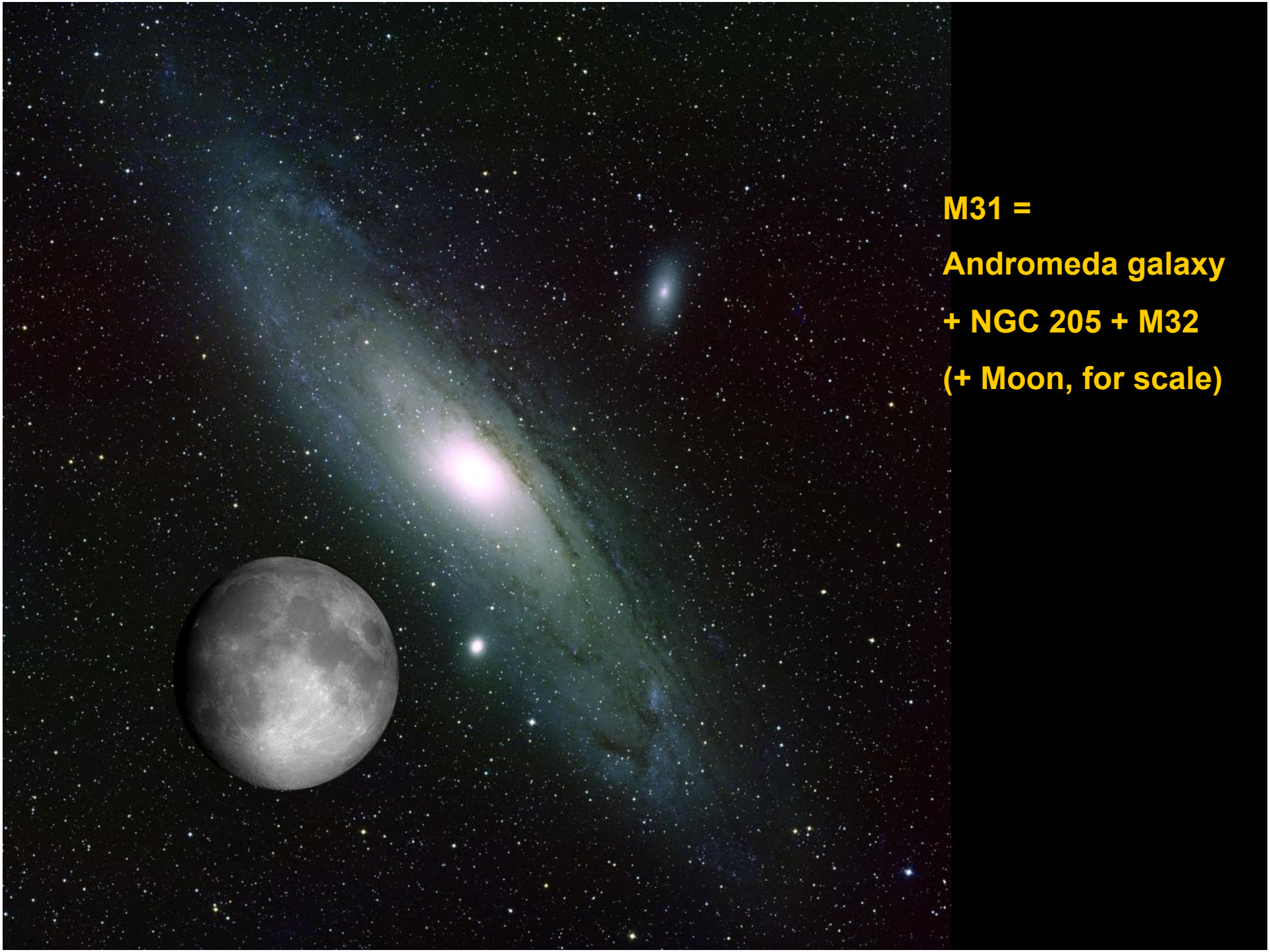
M31 =
Andromeda galaxy
+ NGC 205 + M32
(+ Moon, for scale)

Center of the Milky Way in near-infrared

6 light-months = 4”

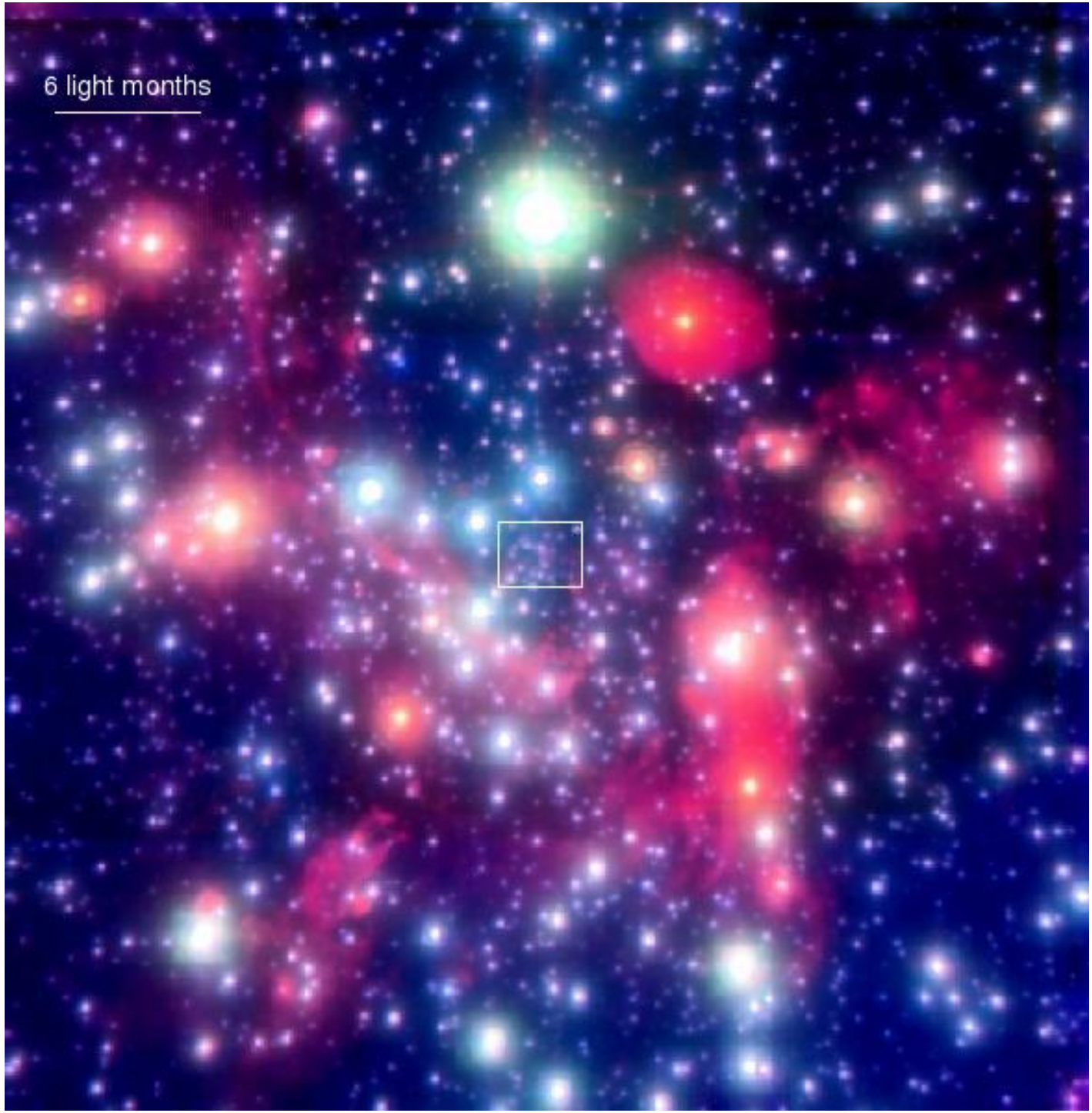

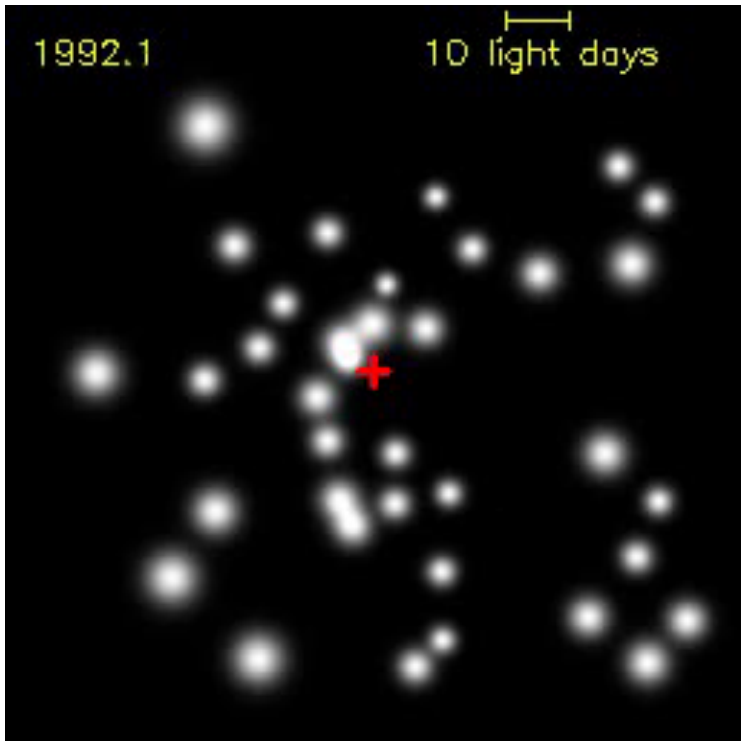
1992.1
10 light days

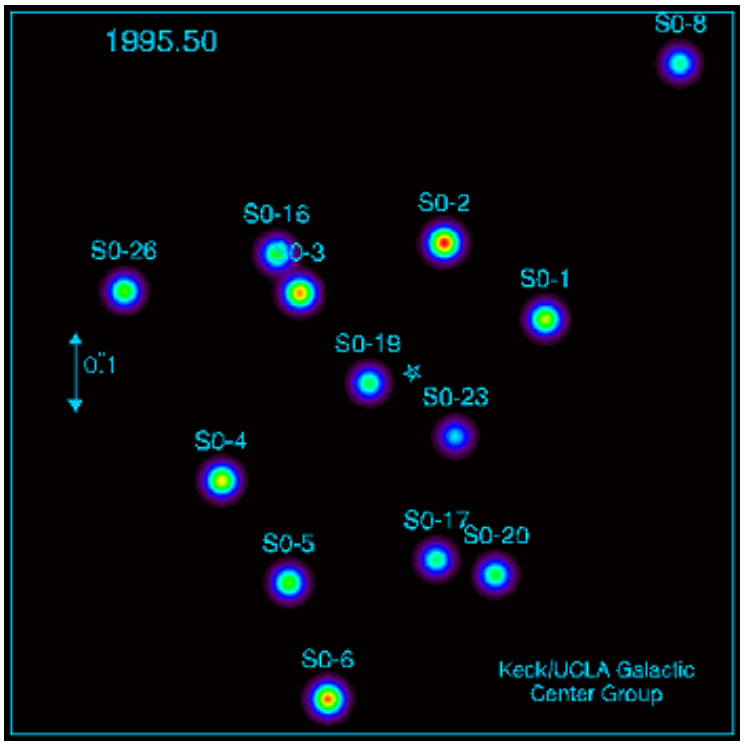
1995.50
S0-8
S0-16
S0-2
S0-26
S0-3
S0-1
0.1
S0-19
S0-23
S0-4
S0-17
S0-20
S0-5
S0-6
Keck/UCLA Galactic
Center Group

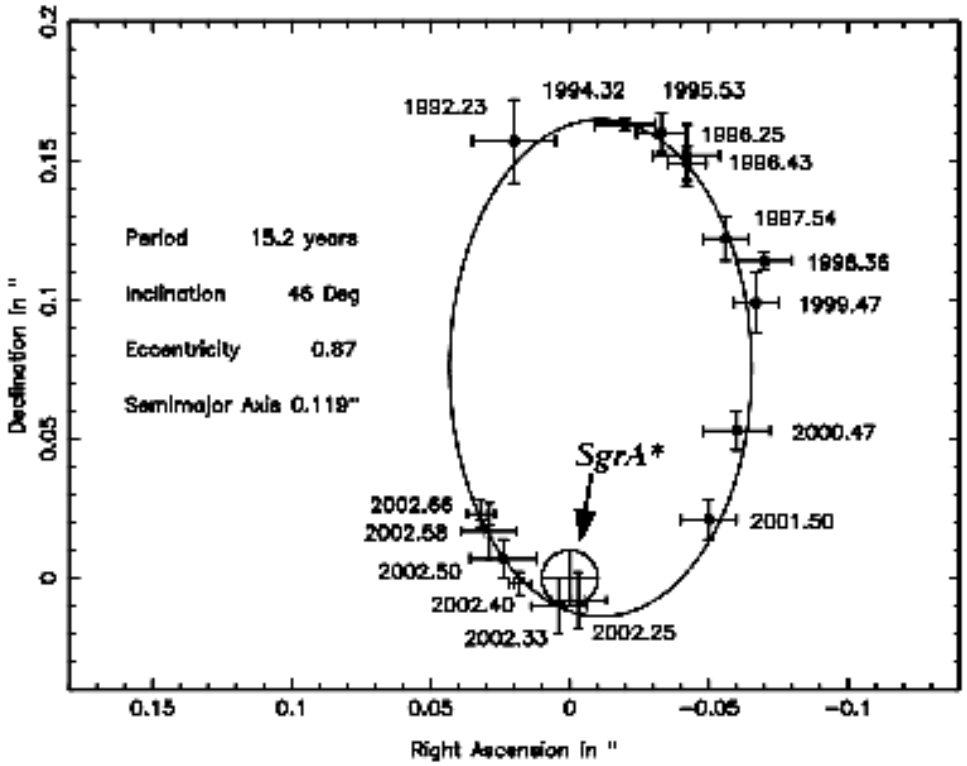

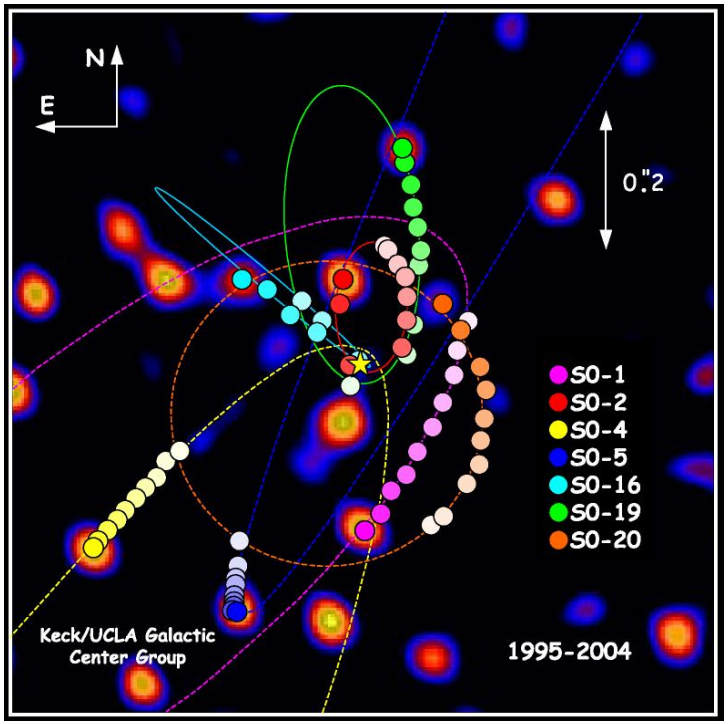

Semimajor axis = 950 AU

Pericenter = 120 AU

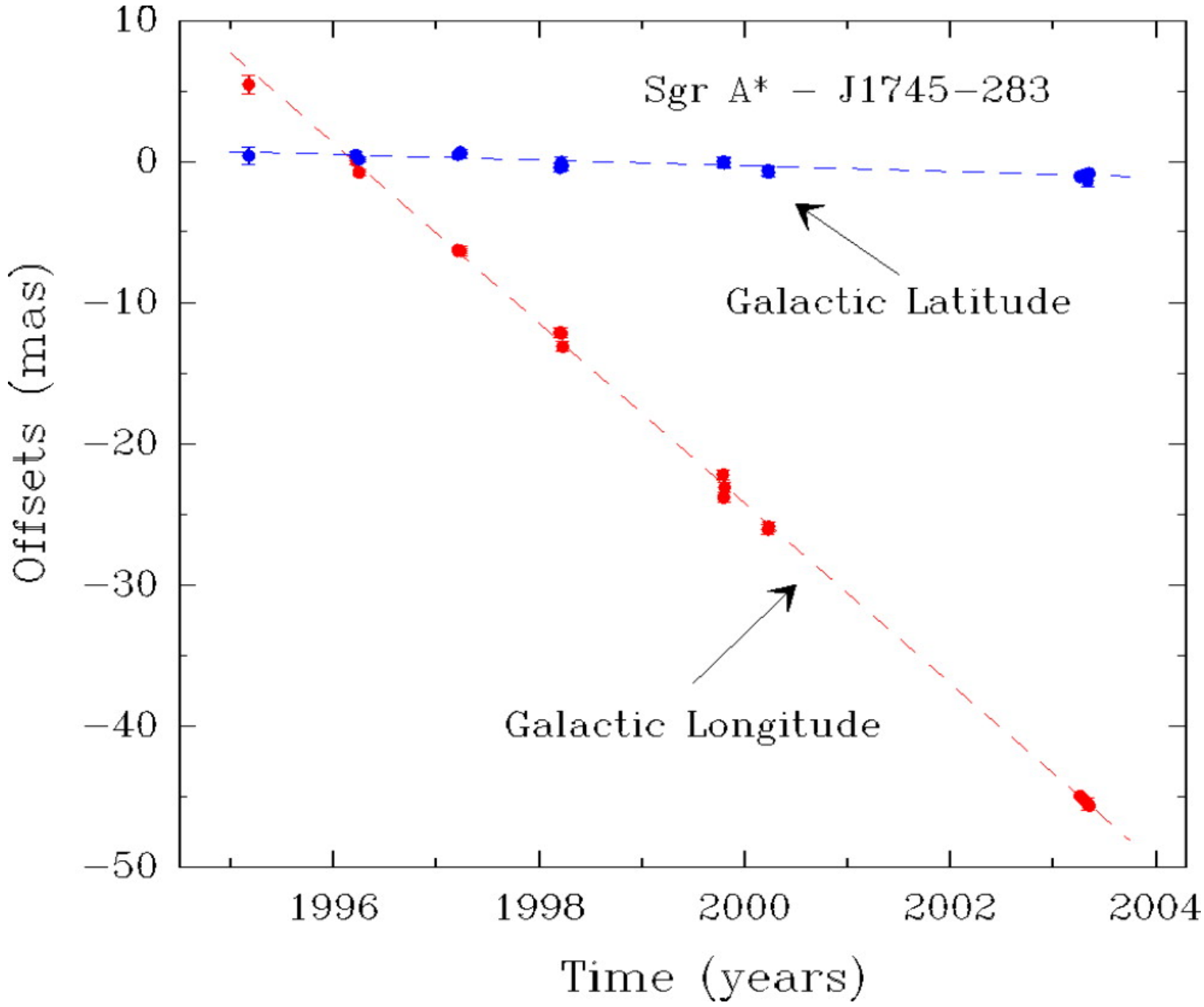

Proper motion (angular speed) of Sgr A*

happens to be the photometric outer edge of the system. If the H I rotation curve is correct, then there must be undetected matter beyond the optical extent of NGC 300; its mass must be at least of the same order as the mass of the detected galaxy. There is no optical rotation data for NGC 300.

d) M33

For $\alpha = 0.13$ per minute of arc (de Vaucouleurs 1959*b*), the theoretical $R_T = 17'$. Optical velocity data by Carranza *et al.* (1968) show a complex velocity field and do not define a unique rotation curve. The rotation curve derived by Mayall and Aller (1942) from velocities of H II regions has R_T at 17′. Brandt's (1965) optical velocities combined with low-resolution 21-cm velocities have $R_T \approx 25'$; this is consistent with the 21-cm data given by Burke, Turner, and Tuve (1963). As in NGC 300, the value of R_T is of the same order as the optical semimajor axis $a \approx 35'$ (de Vaucouleurs 1959*b*).

For two of four systems with weak spheroidal components, the LMC and the SMC, the turnover radii of the rotation curves predicted from the photometrically derived gradients α appear to be consistent with those observed. For NGC 300 and M33, the 21-cm data give turnover points near the photometric outer edges of these systems. These data have relatively low spatial resolution; if they are correct, then there must be in these galaxies additional matter which is undetected, either optically or at 21 cm. Its mass must be at least as large as the mass of the detected galaxy, and its distribution must be quite different from the exponential distribution which holds for the optical galaxy.

APPENDIX B

PHOTOMETRIC PARAMETERS FOR OUR GALAXY

Several authors have constructed mass-distribution models for the Galaxy: these models reproduce the galactic rotation curve, the observed local total density, and some features of the

Freeman (1970)

Rogstad & Shostak (1972)

jects, the constancy of R_{80}/R_{opt} indicates that the light and H I distributions scale together.

f) The rotation curves exhibit steep central gradients and flat outer regions and are all of similar shape. A normalized rotation curve for Scd galaxies, produced by averaging the curves of figure 1 with weights appropriate to the resolution used in their determination, can be very closely represented by a Brandt curve (Brandt and Scheer 1965) with $n = 1.0$, $R_{TO} = 0.6R_{80}$. The mass interior to R_{80}, as computed from equation (2), is $M = 1.5 \times 10^5 R_{80} V_{max}^2$ solar masses with R_{80} in kpc and V_{max} in km s^{-1}. The implied mass distribution is centrally peaked, but decreases only slowly at large radii ($\rho \sim r^{-2}$). Therefore, estimates of the total masses to infinite radius represent a dubious extrapolation of the data.

While resolution effects have probably reduced the derived central velocity gradients, they are nonetheless considerably steeper than those obtained in previous low-resolution H I studies. Consequently, the present results reduce the discrepancy that has appeared to exist between the gradients derived from optical and H I observations.

g) The range in maximal rotation velocity V_{max} is 100 km s^{-1}, and therefore this quantity is not a sensitive classification criterion. Yet the mean value of V_{max} over the galaxies within each class has been shown to decrease with later type (Brosche 1971), and this fact is used to support the hypothesis that, for galaxies of the same mass, the Hubble sequence is an angular-momentum sequence.

We note a remarkably tight linear correlation between the observables R_{opt} and V_{max} for the present galaxies (fig. 2). If this correlation is real, then the Scd mass sequence is completely defined by one parameter. A similar correlation for other classes, if it exists, combined with other results of this paper, would allow complete description of the gross properties of galaxies with only two parameters: angular momentum (Hubble class) and mass (R_{opt} or V_{max}).

which overlap this region and extend the rotation curve to ~29 kpc (Roberts and Whitehurst, 1972). The M 101 rotation curve is from Rogstad and Shostak (1972) and is based on aperture synthesis observations with 4′ resolution made by Rogstad and Shostak (1971) and interpreted by Rogstad (1971). The M 101 curve is typical of those Scd galaxies studied by Rogstad and Shostak (1972) and by Gordon (1971). Pertinent parameters describing each of these galaxies are listed in Table 1.

The rotation curve generally adopted for our Galaxy (Schmidt, 1965) is also shown in Fig. 1. It should be noted that the outer part of the curve is not observationally determined. It is based on an assumed mass model.

Systematic differences among these rotation curves are clearly present. They reflect differences in the mass distribution within each of the galaxies. The more centrally condensed system is the earlier one. Parameters describing the mass distribution are given in Table 2. They are derived for (1) a two-component mass model having a central, spherical, gaussian density distribution and a flat disk with a density distribution according to Toomre's (1963) Model 1 and (2) a flat disk only. The correlation of mass concentration with structural type is insensitive to the model. The detailed description of the mass distribution does, of course, reflect the assumed model. As an example the masses given in Table 2 vary by up to 20% for the two models considered. For the present purpose we do not wish to stress the details of the mass distribution.

The correlation with type is also a correlation with the luminosity distribution. Thus the mass and luminosity distributions vary in the same sense from one galaxy type to another with both distributions more centrally condensed in the earlier type. Although the sample here is woefully small, this conclusion has not, to our knowledge, been established before. It is, however, often assumed to hold.

The three galaxian rotation curves decline slowly, if at all, at large radii implying a significant mass density at these large distances. It is unreasonable to expect the last measured point to refer to the "edge" of the galaxy, and we must conclude that spiral galaxies must be larger than indicated by the usual photometric measurements. This evidence for larger spirals should not be considered a surprise for there is no direct (or indirect) evidence to favor "small" over "large" galaxies. The view favoring the former may possibly be traced to the assumption of a constant mass-to-luminosity ratio with radius. This is far from the case, see e.g. Rubin and Ford (1970). The present data also require that the mass-to-luminosity ratio vary with radius increasing with distance from the center. The range of values is easily compatible with a reasonable variation in the regional luminosity function. This change with radius is in the same sense as that found to occur locally with a change in height above the plane (Bok and MacRae, 1941).

The indication that mass distribution varies with

Roberts & Rots (1973)

Van Albada et al. (1985)

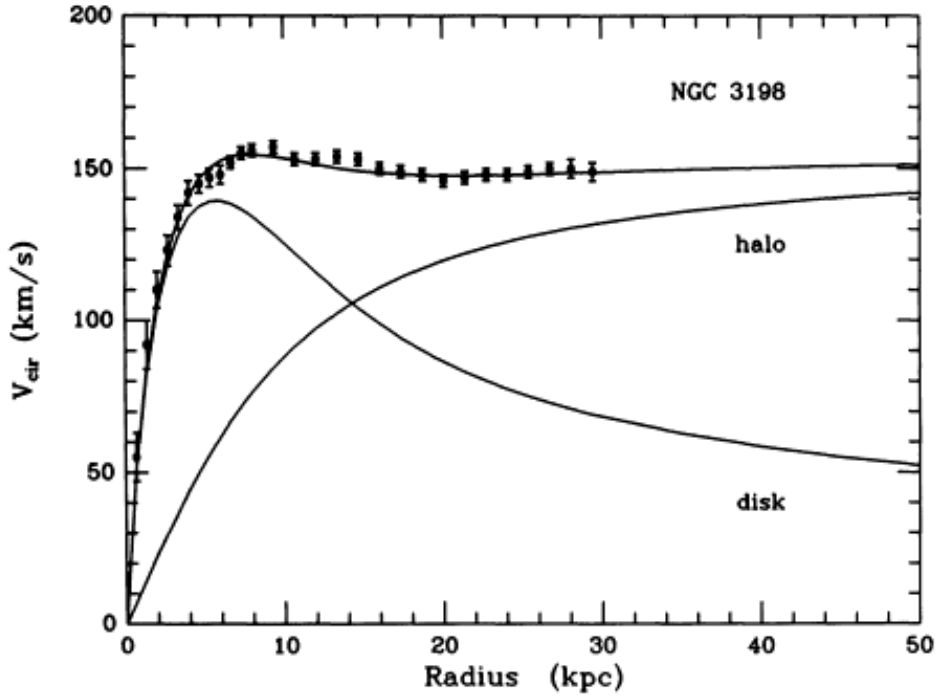

why doesn't "disk" plus "halo" add up to total?

FIG. 4.—Fit of exponential disk with maximum mass and halo to observed rotation curve (*dots with error bars*). The scale length of the disk has been taken equal to that of the light distribution (60", corresponding to 2.68 kpc). The halo curve is based on eq. (1), $a = 8.5$ kpc, $\gamma = 2.1$, $\rho(R_0) = 0.0040\ M_\odot\ \mathrm{pc}^{-3}$.

dark matter to visible matter inside the last point of the rotation curve (at 30 kpc) is 3.9. The enclosed halo mass is 0.8 times the disk mass at R_{25}; the enclosed halo mass is 1.5 times the disk mass at the Holmberg radius. The total mass inside 30 kpc is $15 \times 10^{10}\ M_\odot$. Another property of interest is the mass-to-light ratio of the disk; we find $M/L_B(\mathrm{disk}) \leq 3.6\ M_\odot/L_{B_\odot}$ and $M/L_V(\mathrm{disk}) \leq 4.4\ M_\odot/L_{V_\odot}$.

The disk-halo model shown in Figure 4 has the characteristic flat rotation curve over a large part of the galaxy. Beyond 30 kpc it is a mere extrapolation, but the observations inside 30 kpc do not show any sign of a decline, and the extrapolated curve may well be close to the true one. To obtain an estimate of the minimum amount of dark matter at large distances from the center we have also made a fit, shown in Figure 6, with a halo density law whose slope changes from -2 in the inner region to -4 in the outer region:

$$\rho_{\mathrm{halo}}(R) \propto \left[\left(\frac{a}{R_0}\right)^2 + \left(\frac{R}{R_0}\right)^2 + 0.08\left(\frac{R}{R_0}\right)^4\right]^{-1}, \qquad (2)$$

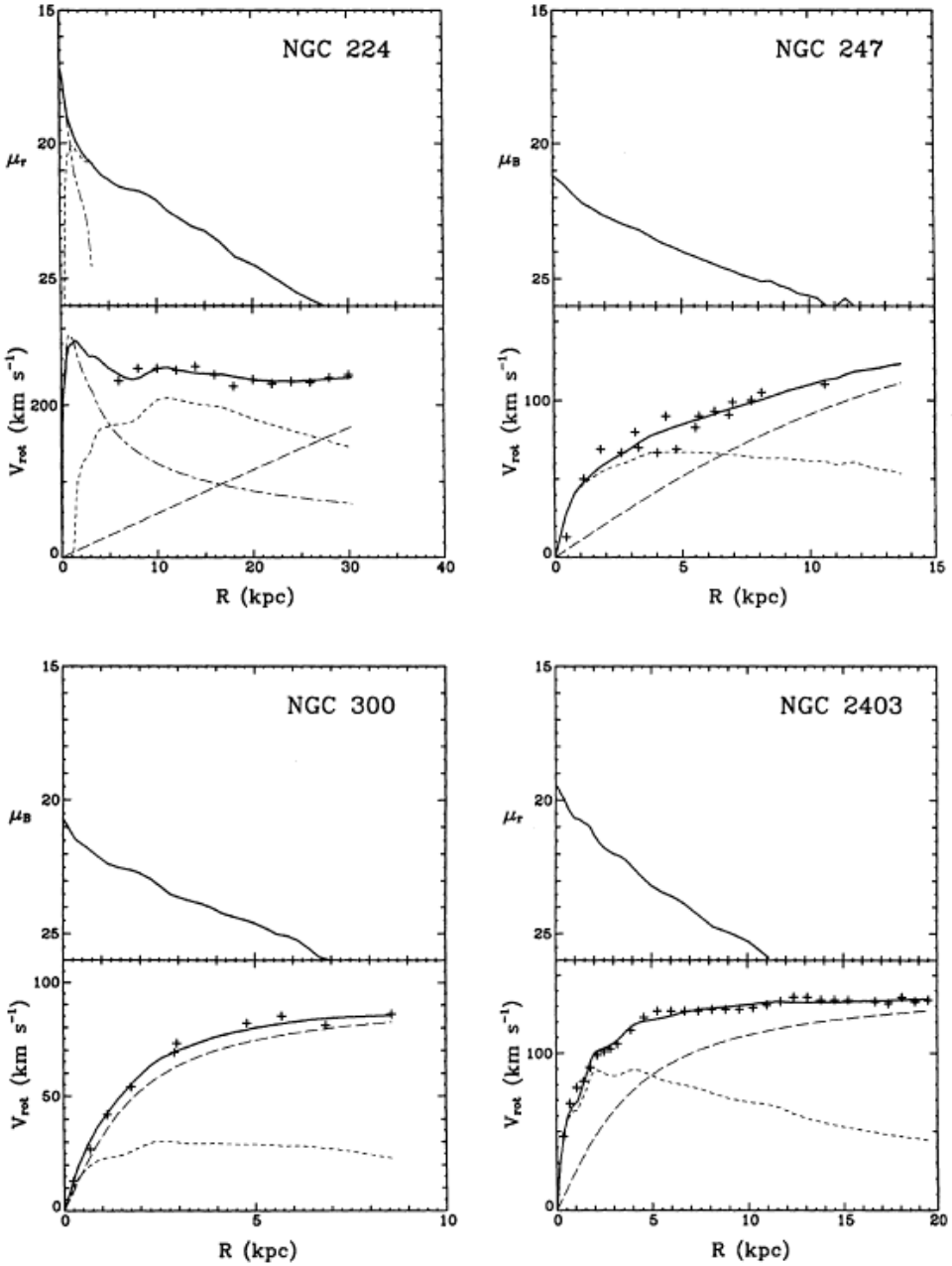

FIG. 1. Top panels: major-axis luminosity profiles for 16 spiral galaxies. The profile is decomposed into bulge (short- and long-dashed) and disk (short-dashed) components. Lower panels: observed rotation curves (pluses) and the best-fitting full solution (solid line). The separate contributions of the bulge, disk, and halo are also drawn.

Kent (1987)

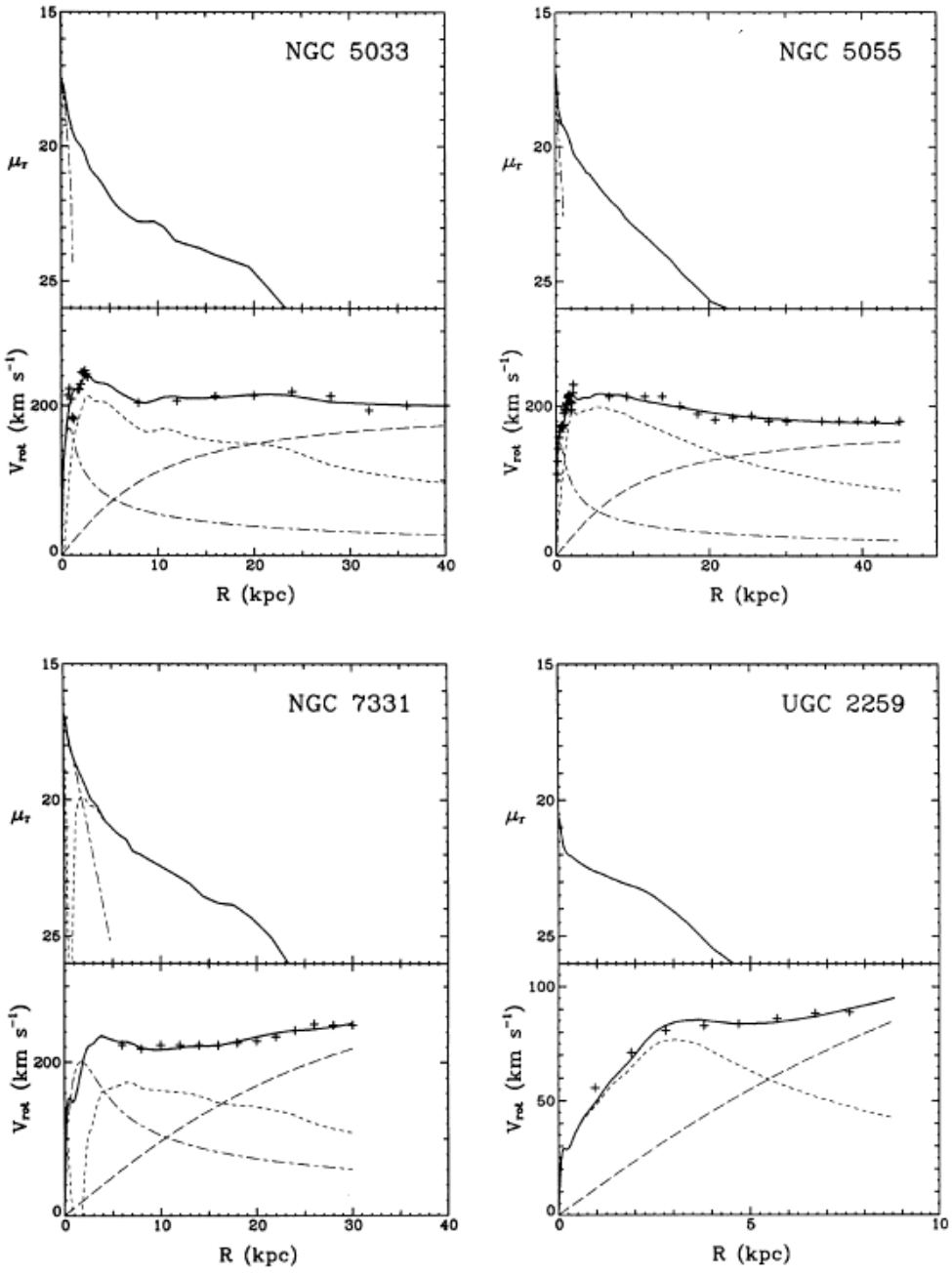

FIG. 1. (continued)

Kent (1987)

THE ASTROPHYSICAL JOURNAL, 193:L1–L4, 1974 October 1

THE SIZE AND MASS OF GALAXIES, AND THE MASS OF THE UNIVERSE

J. P. OSTRIKER
Princeton University Observatory

P. J. E. PEEBLES
Joseph Henry Laboratories, Princeton University

AND

A. YAHIL
Princeton University Observatory; and Department of Physics, Tel-Aviv University
Received 1974 May 28; revised 1974 July 15

ABSTRACT

Currently available observations strongly indicate that the mass of spiral galaxies increases almost linearly with radius to nearly 1 Mpc. This means that the total mass per giant spiral is of the order of $10^{12}\ M_\odot$, and that the ratio of this mass to the photographic light within the Holberg radius, f, is $\sim 200\ (M/L)_\odot$. Using this value of f and the luminosity function of surveyed galaxies, we determine a local mean cosmological mass density $\approx 2 \times 10^{-30}$ g cm^{-3} corresponding to $\Omega = \rho/\rho_{crit} \approx 0.2$. The uncertainty in this result is not less than a factor of 3.

Subject headings: cosmology — galactic structure

I. THE ARGUMENT

There are reasons, increasing in number and quality, to believe that the masses of ordinary galaxies may have been underestimated by a factor of 10 or more. Since the mean density of the Universe is computed by multiplying the observed number density of galaxies by the typical mass per galaxy, the mean mass density of the Universe would have been underestimated by the same factor. Finally, the current estimate (Shapiro 1971) for the ratio of gravitational energy to kinetic energy in the Universe is about $\Omega = 0.01$. If we increase the estimated mass of each galaxy by a factor well in

the disk mass exterior to the Sun ($r > 10$ kpc) and almost no information about the exterior halo mass. Similarly the studies by Page (1961) of galaxies' masses in binary pairs contain little information concerning distributed mass with a scale greater than the typically $\sim$30 kpc separation.

This ignorance would give us little cause for concern if we had reason to believe from measurements with $r < 20$ kpc that the mass $M(r)$ had "converged" to some limiting value. However, this is not the case; available evidence, summarized below, indicates that the measured masses of galaxies diverge with increasing distance even though the luminosities of the flattened

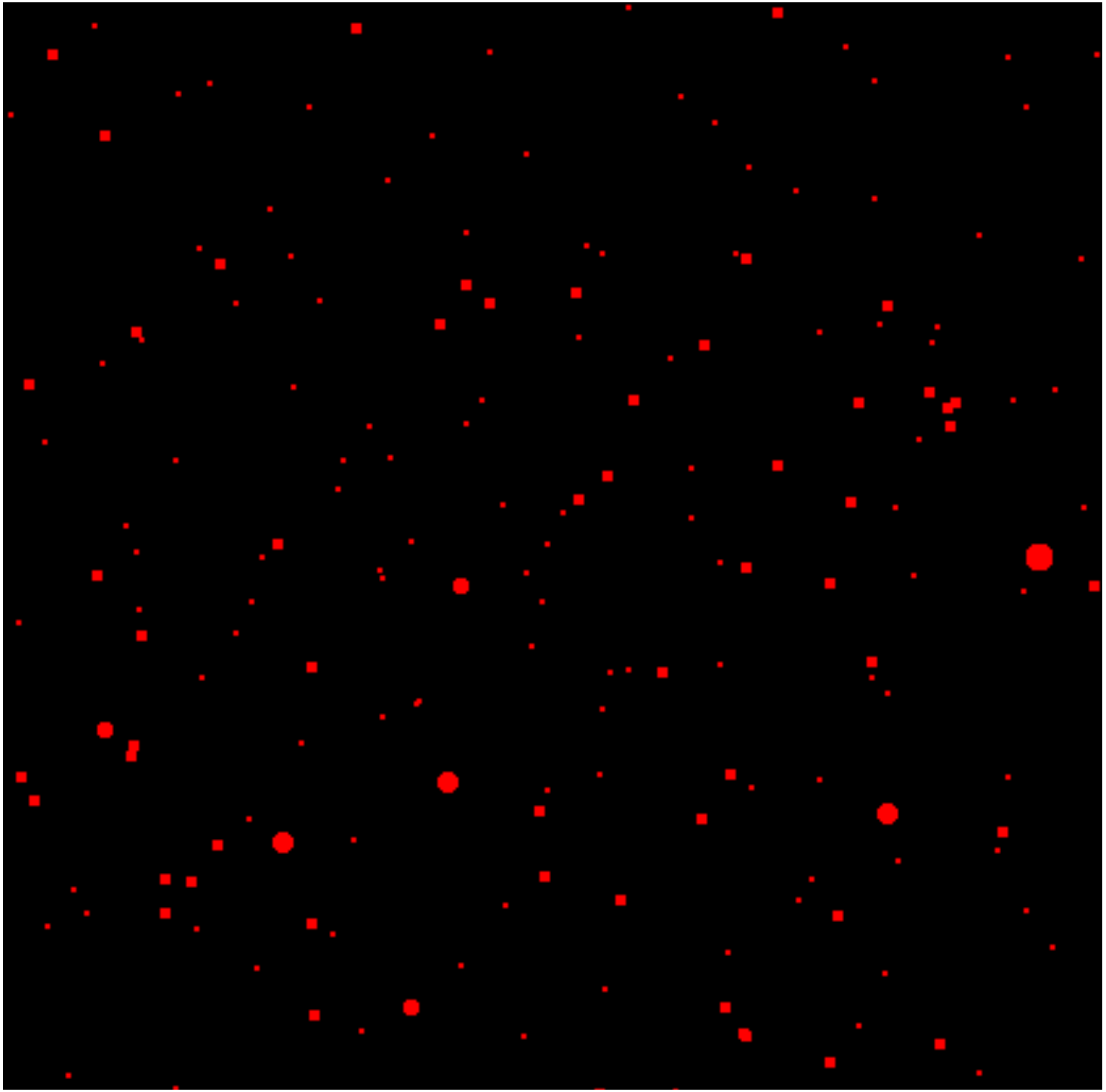

Hipparcos animation of 8X8 degree field over 1500 yr

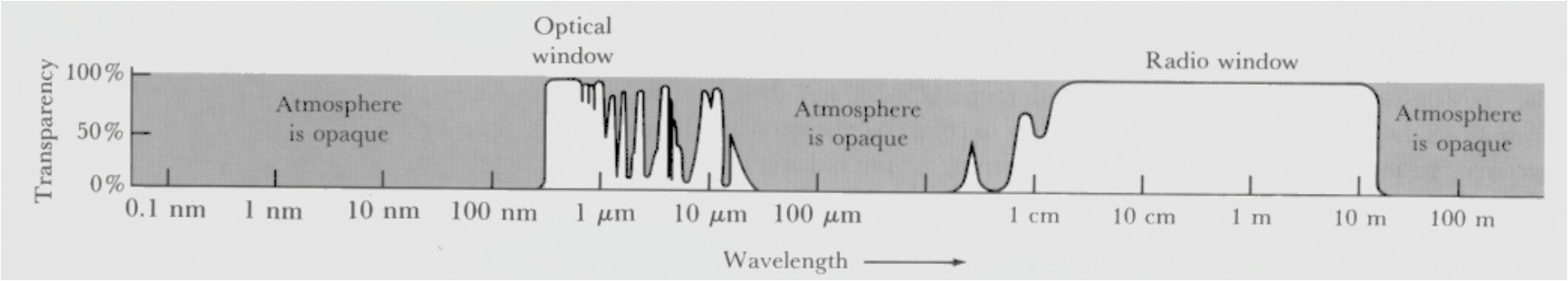
Optical
window
Radio window
Transparency
100%
50%
0%
Atmosphere
is opaque
Atmosphere
is opaque
Atmosphere
is opaque
0.1 nm
1 nm
10 nm
100 nm
1 μm
10 μm
100 μm
1 cm
10 cm
1 m
10 m
100 m
Wavelength

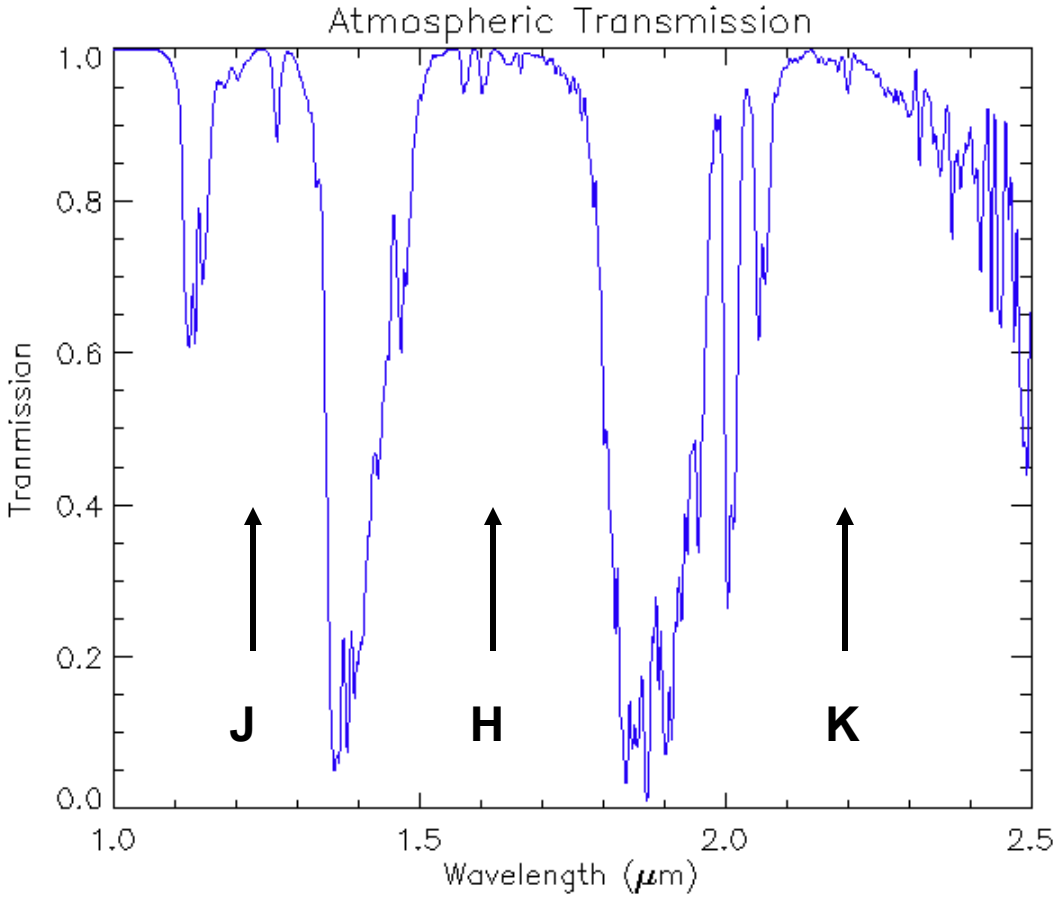
Atmospheric Transmission
Tranmission
1.0
0.8
0.6
0.4
0.2
0.0
J
H
K
1.0
1.5
2.0
2.5
Wavelength (μm)

Ten nearest stars

name	M_V	d (pc)
Prox Cen	15.53	1.30
α Cen A	4.38	1.34
α Cen B	5.71	1.34
Barnard's star	13.22	1.83
Wolf 359	16.55	2.39
Lalande 21185	10.44	2.54
Sirius	1.47	2.63
UV Ceti	15.40	2.67
BL Ceti	15.85	2.67
Ross 154	13.07	2.97

Ten brightest stars

name	M_V	d (pc)
Sirius	1.4	2.63
Canopus	-2.5	36
Arcturus	0.2	103
α Cen A	4.38	1.34
Vega	0.6	7.5
Capella	-0.4	12.5
Rigel	-8.1	7.7
Procyon	2.7	3.42
Achemar	-1.3	38
Betelgeuse	-7.2	200

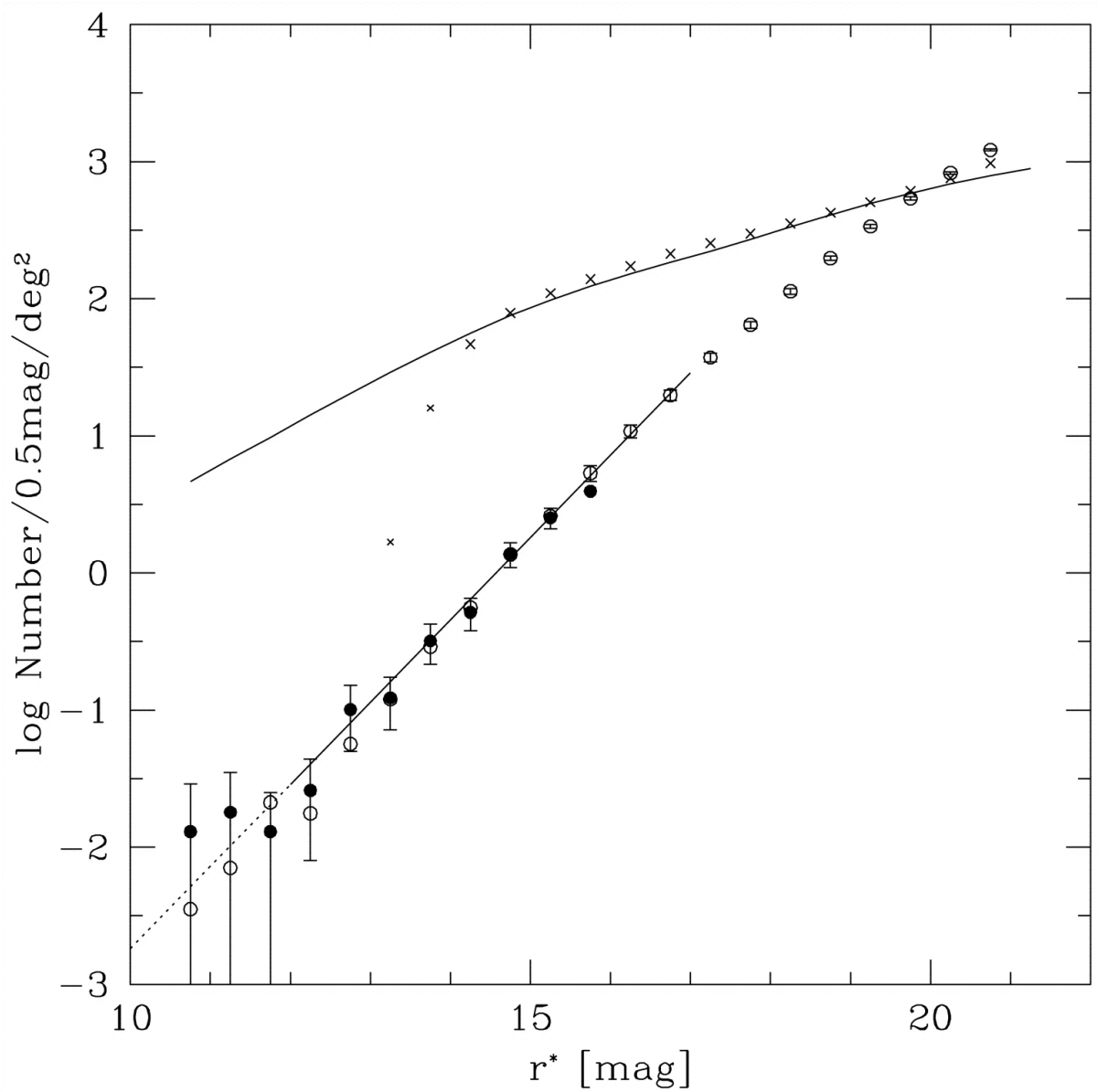

SDSS galaxy counts

Yasuda et al. (2001)

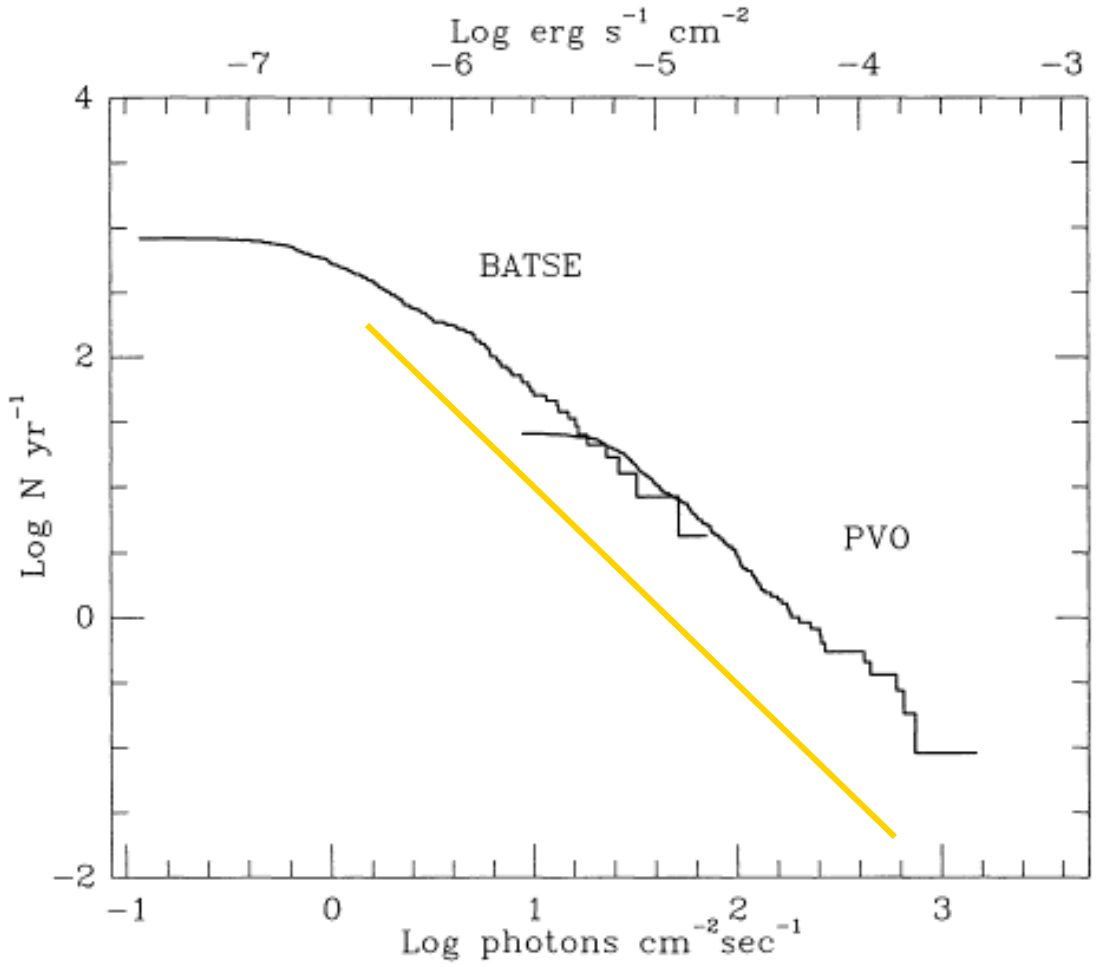

Figure 13 The log N–log P distribution from combined BATSE and *PVO* data (adapted from Fenimore et al 1993). The distributions match well in the overlap region. The *PVO* data, which has recorded more strong bursts than BATSE during its long lifetime, is seen to follow a −3/2 power law for strong bursts.

Gamma-ray burst counts

Fishman & Meegan (1995)

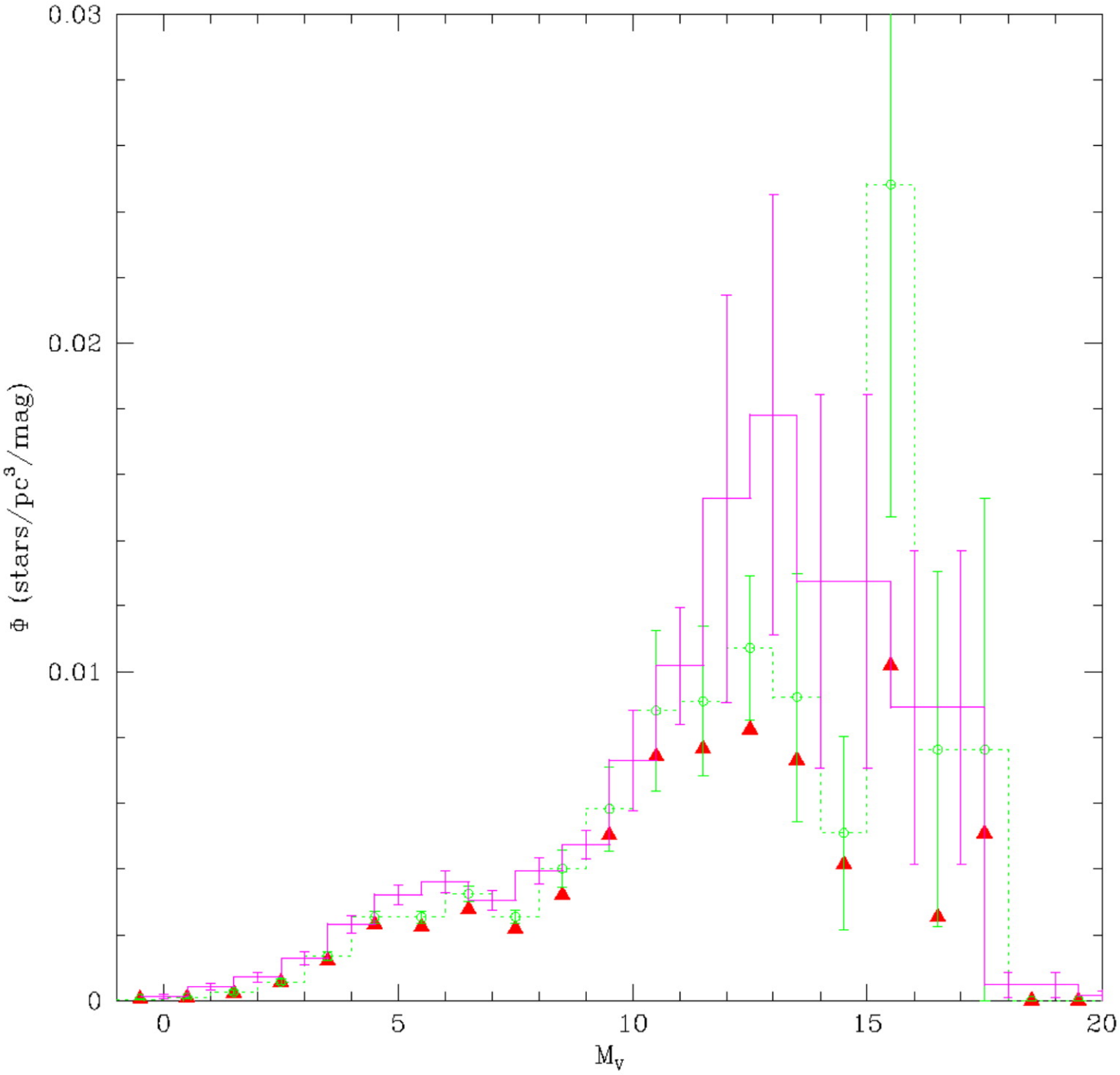

Reid et al. (2002)

red = no correction for binaries

green = corrected for binaries

purple = Wielen et al. (1983)

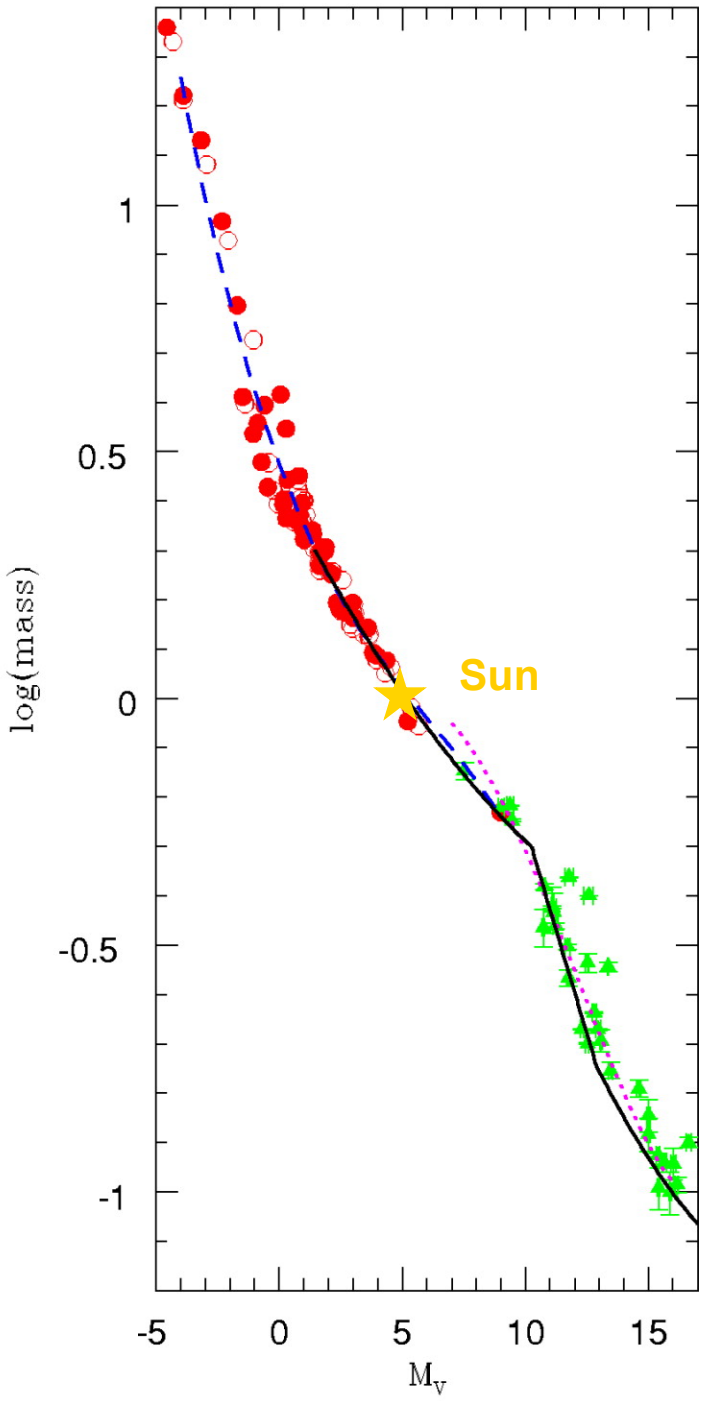

The mass-luminosity relation for main-sequence stars

(Reid et al. 2002)

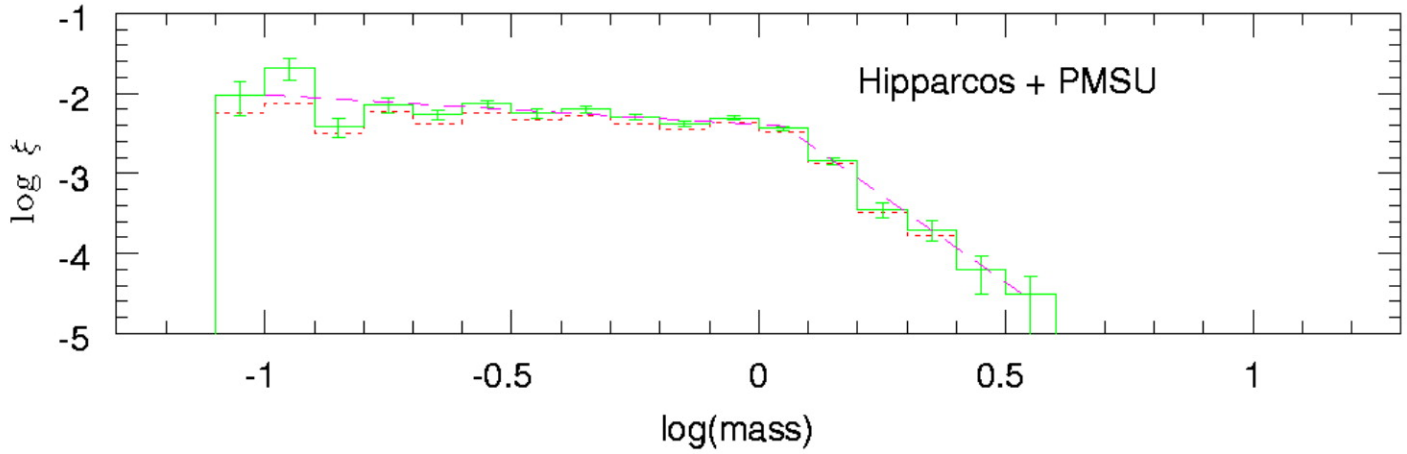

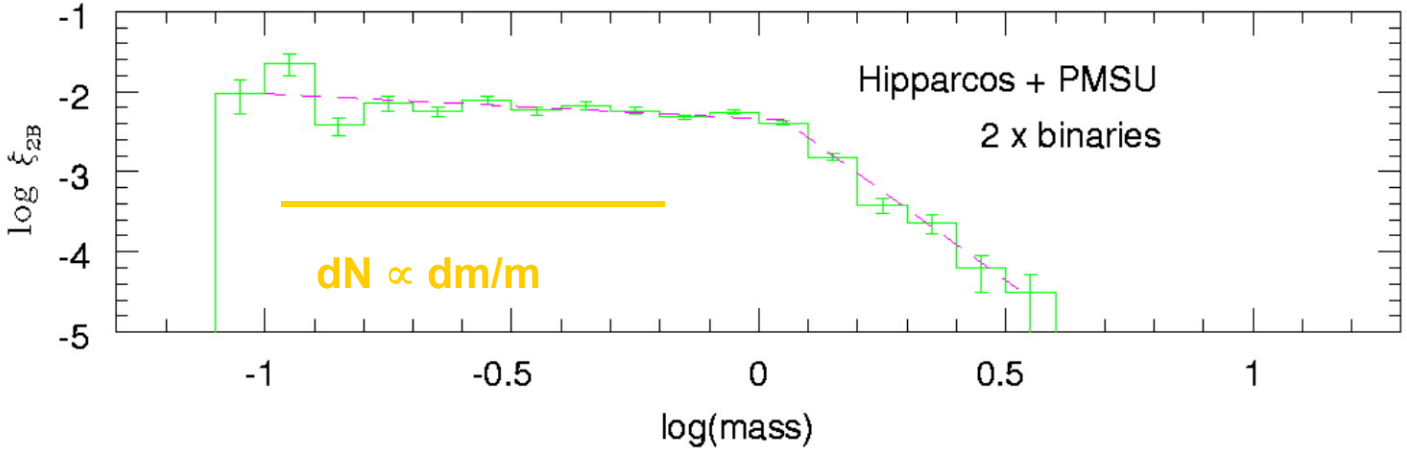

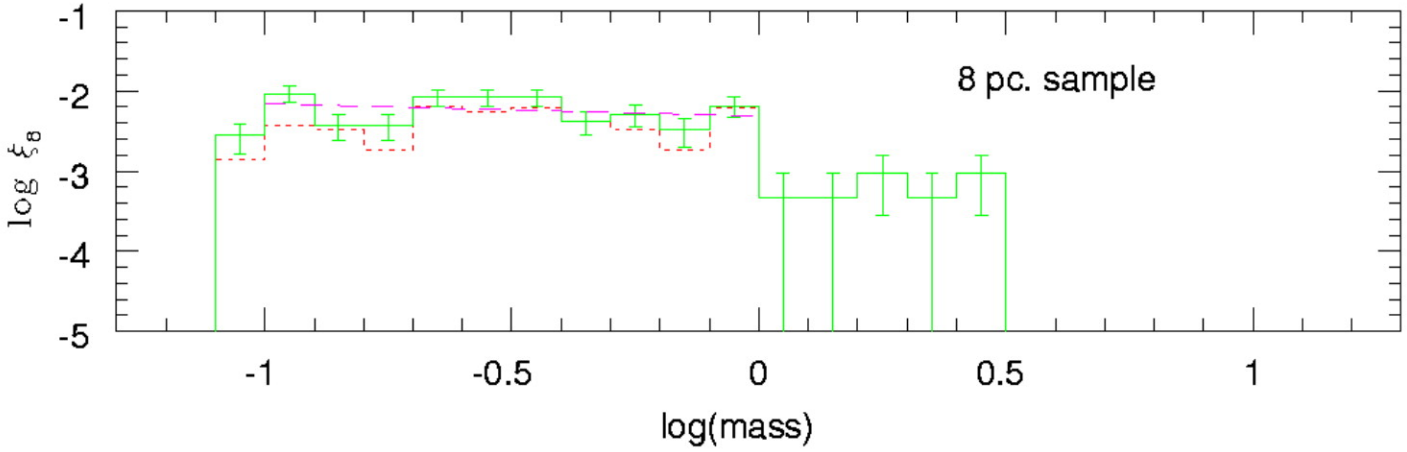

Mass function in the solar neighborhood

dN = ξ(m) d log m = n(m)dm

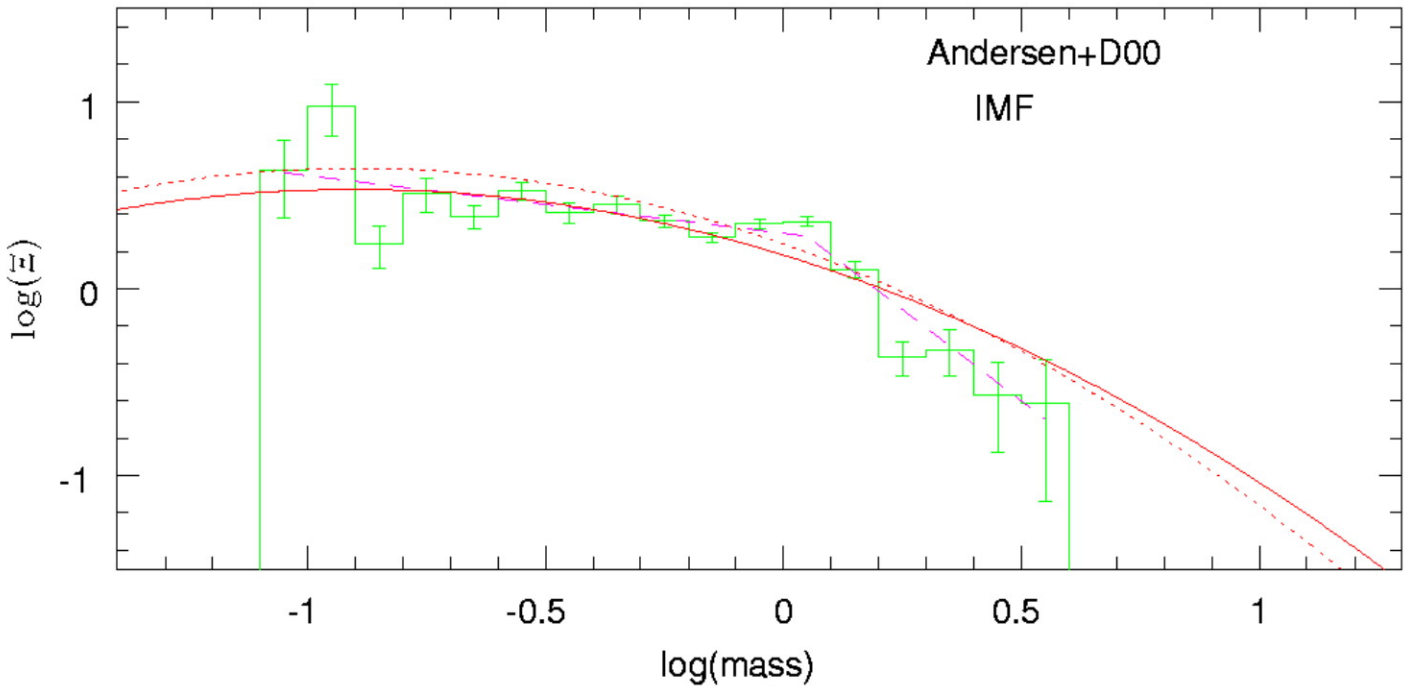

Initial mass function in the solar neighborhood

dN = ξ(m) d log m = n(m)dm

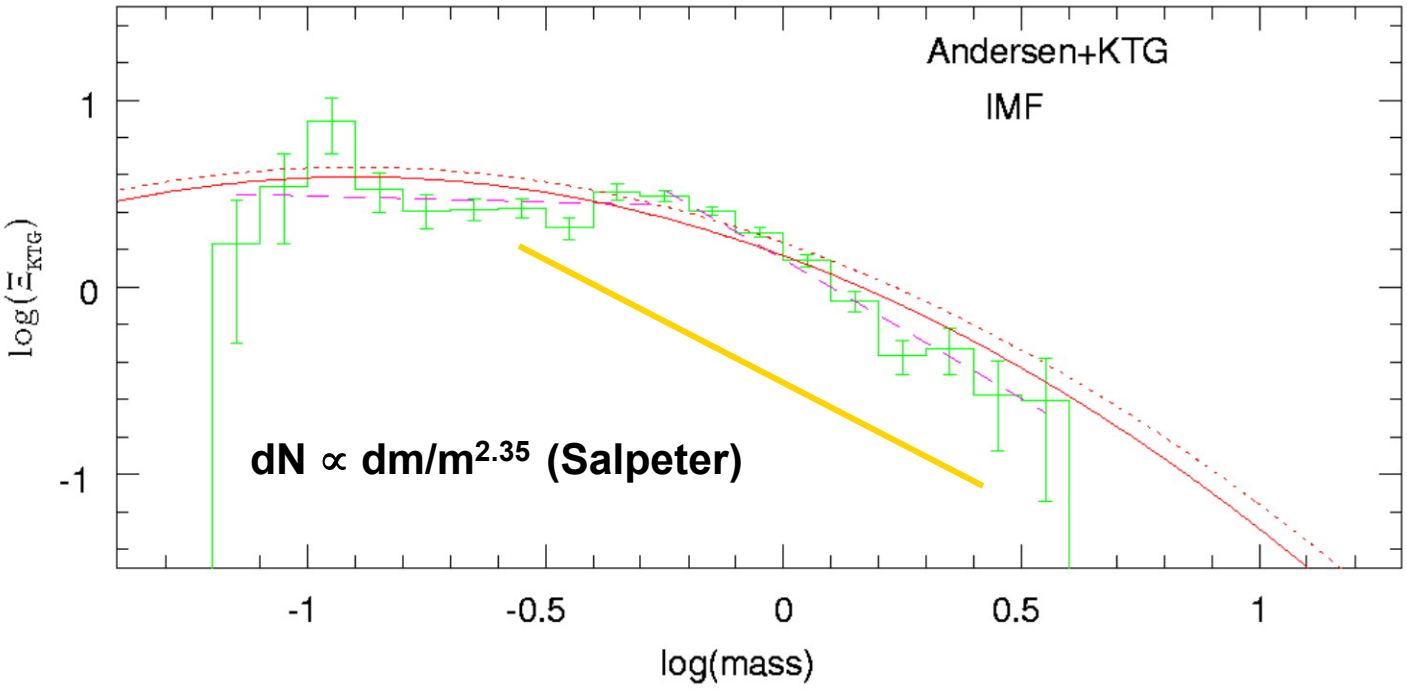

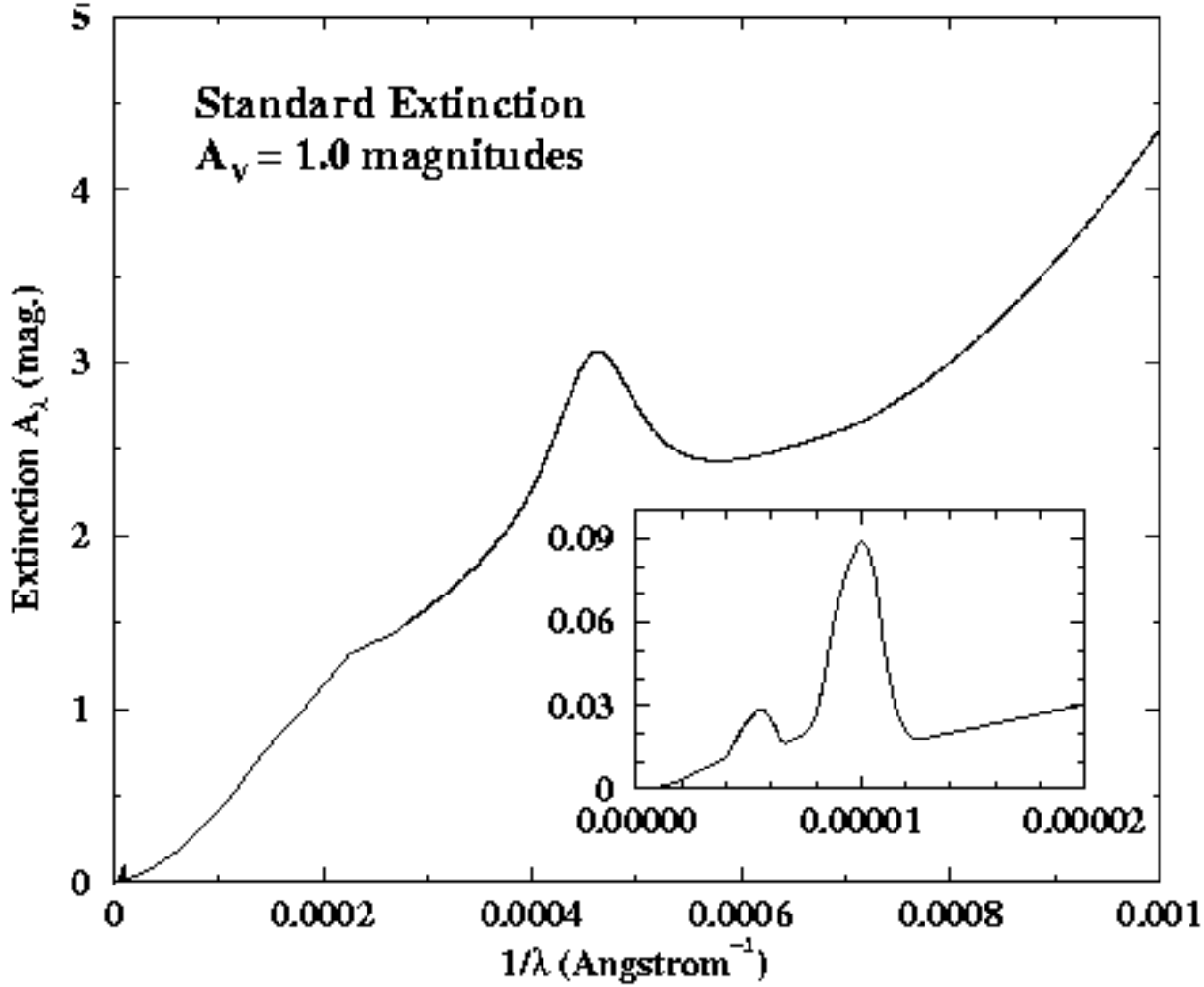
Standard Extinction
$A_V = 1.0$ magnitudes
Extinction A_λ (mag.)
$1/\lambda$ (Angstrom^{-1})
0
1
2
3
4
5
0
0.0002
0.0004
0.0006
0.0008
0.001
0.09
0.06
0.03
0
0.00000
0.00001
0.00002

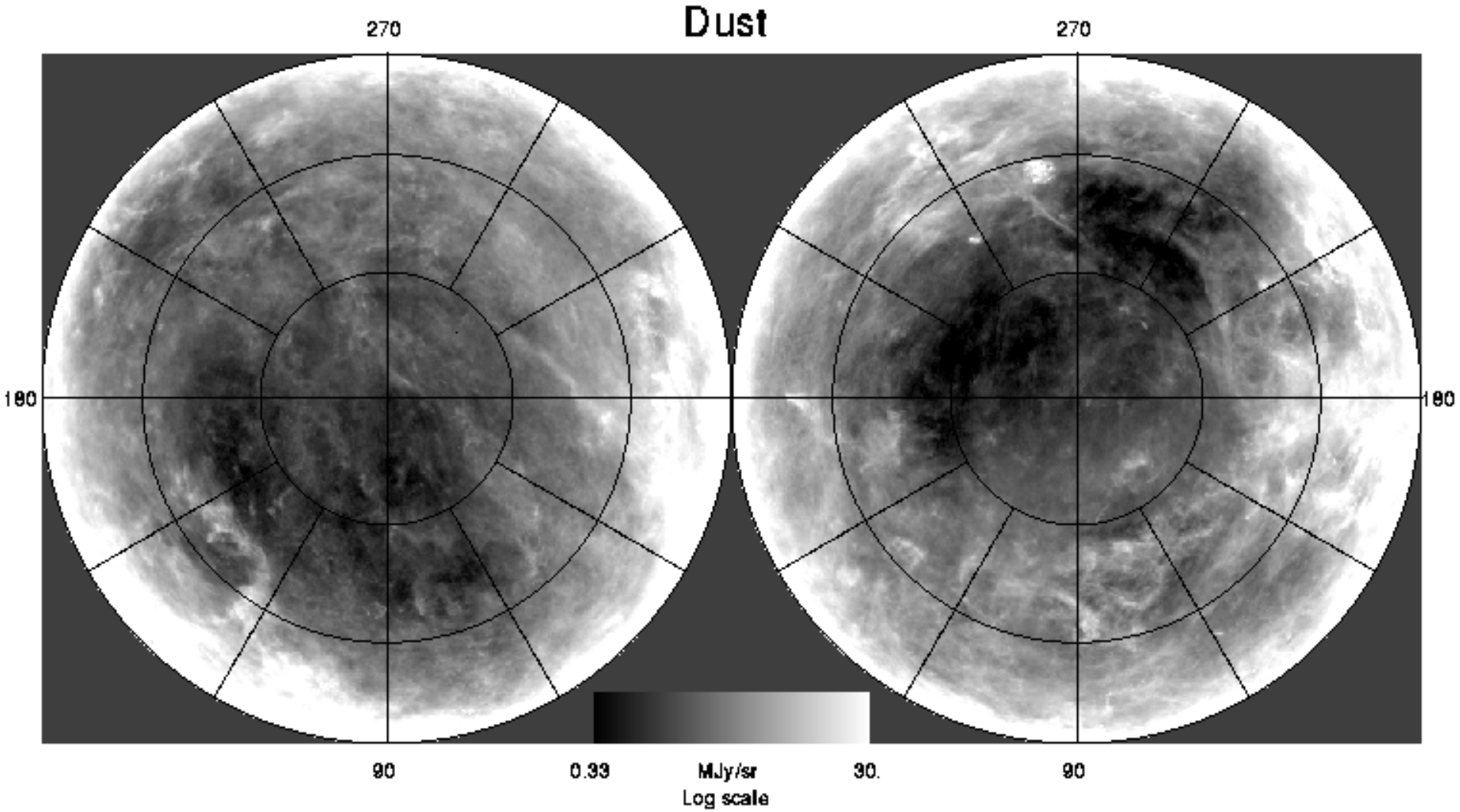

Schlegel, Finkbeiner & Davis (1998)